THE ASTROPHYSICAL JOURNAL, 416:554–562, 1993 October 20

MAGNETIC FIELDS IN THE HYDRA A CLUSTER

GREGORY B. TAYLOR
California Institute of Technology, Radio Astronomy, 105-24, Pasadena, CA 91125
AND
RICHARD A. PERLEY
National Radio Astronomy Observatory, P.O. Box 0, Socorro, NM 87801
Received 1993 March 23; accepted 1993 April 27

ABSTRACT

Sensitive, high-resolution VLA polarimetric observations are presented for the radio galaxy Hydra A, an outstanding example of a high-luminosity radio source embedded within a cooling flow cluster. We find extremely high Faraday rotation measures (RMs), throughout the central regions of this source, with a strong asymmetry between the north and south lobes. Simple models for the high RMs are discussed and compared with the observations. To explain the north-south asymmetry in RM requires a magnetic field of strength ~ 6 μG organized over a scale of ~ 100 kpc. On smaller scales we find a tangled magnetic field with a strength of ~ 30 μG.

Subject headings: galaxies: clusters: individual (Hydra A) — intergalactic medium — magnetic fields — polarization

1. INTRODUCTION

Faraday rotation of the plane of polarization by an intervening magnetized plasma offers us a powerful tool for understanding the distribution of magnetic fields and gas lying between us and distant radio sources. Studies of the rotation measure (RM) have shown that a small number of radio sources display extraordinarily high RMs. These objects have quite naturally generated great interest and detailed observations of them have been undertaken in recent years.

So far, 15 such high RM sources have been observed (Ge 1991; Taylor 1991; Taylor, Inoue, & Tabara 1992a). In every case for which good optical data is available, these high RM sources are found to be in clusters. Furthermore, X-ray observations have revealed a copious amount of hot gas in these clusters. The picture that has emerged from these studies is that the high RMs are produced by magnetic fields in the hot gas which surrounds the radio source (Cygnus A, Dreher, Carilli, & Perley 1987; Hydra A, Taylor et al. 1990; 3C 295, Perley & Taylor 1991; A 1795, Ge & Owen 1993). Understanding these cluster magnetic fields, which raise interesting questions about early star and galaxy formation (Pudritz & Silk 1989) and may have significant effects on the evolution of clusters (Sarazin 1986; Soker & Sarazin 1990) is of considerable current interest. RM observations provide information about the density-weighted magnetic field along lines of sight through the cluster to the radio source. Unfortunately, these RM observations can only be feasibly determined for sources with polarized flux densities exceeding ~ 40 μJy beam^{-1} (achievable in 8 hr with the VLA at 3.6 cm). Several of the weaker high RM sources (e.g., A 1795) only meet this criterion in a few places, while many (7/15, or 47%) are CSS sources from which little structural information about the RMs can be derived.

Of the high RM sources, Hydra A is the only source for which RMs have been determined continuously from within a few arcseconds of the radio core, out to a distance of 40″ (55 kpc). Hydra A is unusual in other respects as well, having a radio luminosity an order of magnitude beyond the F-R I/F-R II break despite its F-R I morphology, and with a large angular (8′) and physical size (700 kpc).

2. THE OBSERVATIONS

The detailed RM structure in Hydra A has been the target of two observing campaigns. The results of the first are presented in Taylor et al. (1990). The main results of this study were the discovery of RMs in the north lobe ranging from -1000 to $+3300$ radians m^{-2}, and the discovery of severe depolarization in the south lobe—presumably caused by even larger RMs and RM gradients. To resolve these large RM gradients and unambiguously determine the larger RMs in the south lobe, we reobserved Hydra A with the VLA[1] at four frequencies in the 3.6 cm band. In order to obtain the necessary sensitivity at a high-resolution, full track observations were made in the A, B, C, and D configurations (see Table 1). The data were calibrated, combined and imaged in a similar manner to that described in Taylor et al. (1990). As before, the RM image was obtained by performing a least-squares fit of a λ^2-relation to measurements of the polarization angle at each pixel.

The new RM image derived from these 3.6 cm observations at 0.″3 resolution is in good agreement with the previous RM image in the north lobe. The north lobe has RMs ranging from -1000 to $+3300$ radians m^{-2} (Fig. 1 [Pl. 16]). Several regions with diameters $\sim 3''$ (4.2 kpc) show roughly homogeneous RMs, indicating that the magnetic field producing them is ordered on this scale. Gradients in the RM of 1000 rad m^{-2} over 1″ are observed in the north lobe. The 2 cm and 3.6 cm data are $\sim 50\%$ polarized in the north lobe, while the 6 cm data are $\sim 40\%$ polarized. In the south lobe, the new RM image (Fig. 1) reveals RMs up to $-12{,}000$ radians m^{-2}, values exceeded only in 3C 295 (Perley & Taylor 1991) and OQ 172

[1] The VLA is a facility of the National Radio Astronomy Observatory, is operated by Associated Universities, Inc., under cooperative agreement with the National Science Foundation.

PLATE 16

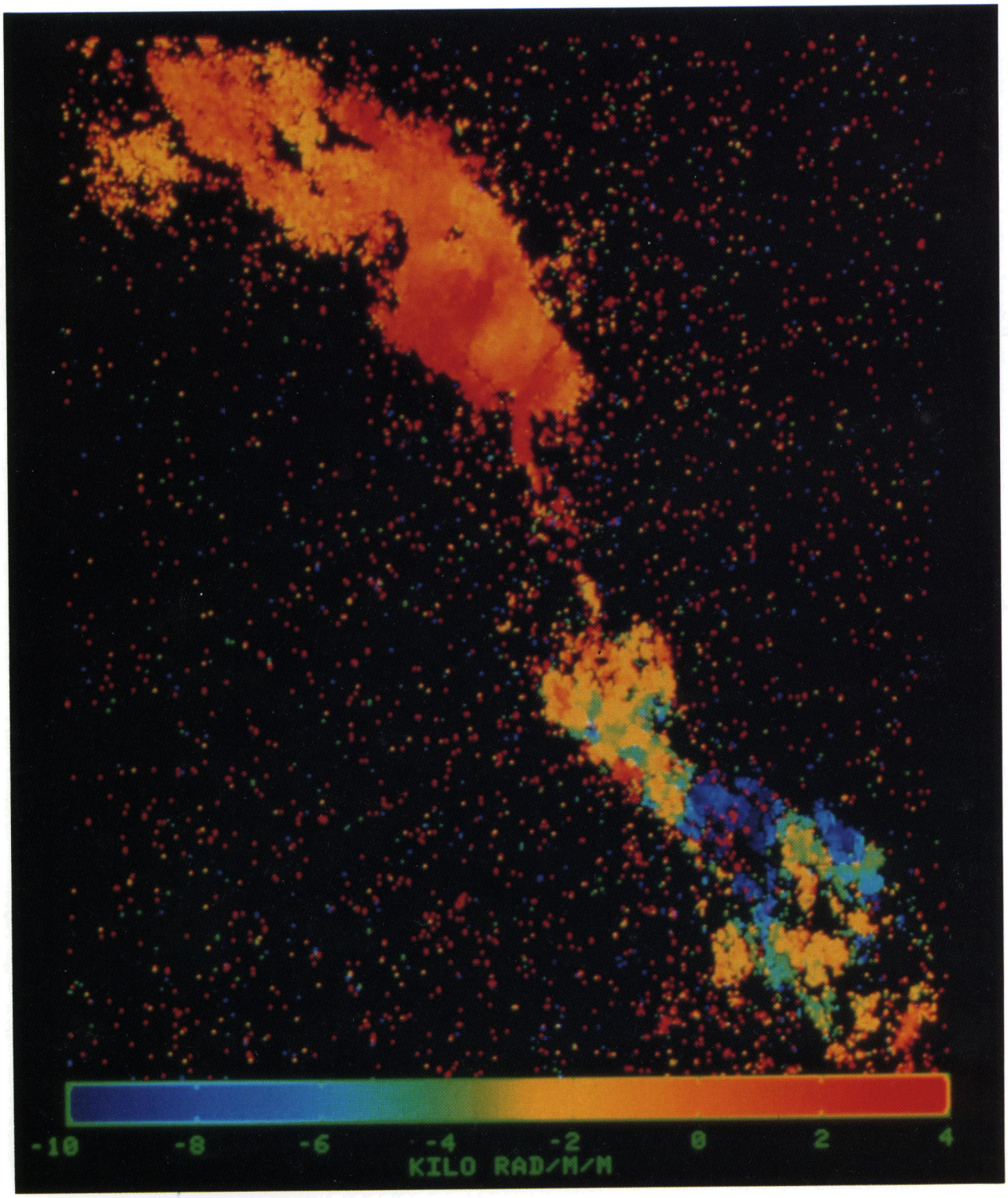

FIG. 1.—The RM structure of Hydra A at 0".3 resolution. This image shows orderly transitions in the north lobe from regions of -1000 to $+3000$ radians m^{-2}. Several regions with nearly uniform RM are seen over patches of size $\sim 3''$ (4 kpc). The RM changes sign about the core from mostly positive in the north to mostly negative in the south. The RMs and gradients in RM are much larger in the south lobe. The colors indicate RMs from $-10{,}000$ to 4000 radians m^{-2}.

TABLE 1

VLA OBSERVATIONS OF HYDRA A AT 3.6 cm

Date	Configuration	Frequencies (MHz)	Duration (hr)	Bandwidth (MHz)
1989 Apr 30	B	7815, 8165	2.88	25.0
		8515, 8885	2.88	25.0
1989 Aug 28	C	7815, 8165	1.55	25.0
		8515, 8885	1.47	25.0
1989 Dec 21	D	7815, 8165	1.25	50.0
		8515, 8885	1.30	50.0
1990 Mar 14	A	7815, 8165	1.81	12.5
		8515, 8885	1.77	12.5
1990 Apr 12	A	7815, 8165	1.81	12.5
		8515, 8885	1.77	12.5

(K. Aizu, private communication). The RM structure of the south lobe appears much more "patchy" than in the north lobe, with a scale size of $\sim 2''$ (2.8 kpc), and the RMs are predominantly negative, while in the north lobe they are predominantly positive. This observation indicates a large-scale (100 kpc) ordering to the cluster magnetic field. Some sample fits in a region of very high RM in the south lobe are shown in Figure 2. This figure shows that the polarization angles in this region are well fitted by a λ^2-relation as is the case for the entire source. The physical conditions necessary to produce such large RMs will be discussed in § 3.

3. SOURCES OF ROTATION MEASURE

In the following sections we discuss the regions that could potentially give rise to the very high RMs observed in Hydra A. Moving from the telescope to the source these are the interstellar medium (ISM) of the Milky Way, the intergalactic medium (IGM), the intracluster medium (ICM), the region of optical-line-emitting gas, a cocoon around the radio source, and the radio source itself.

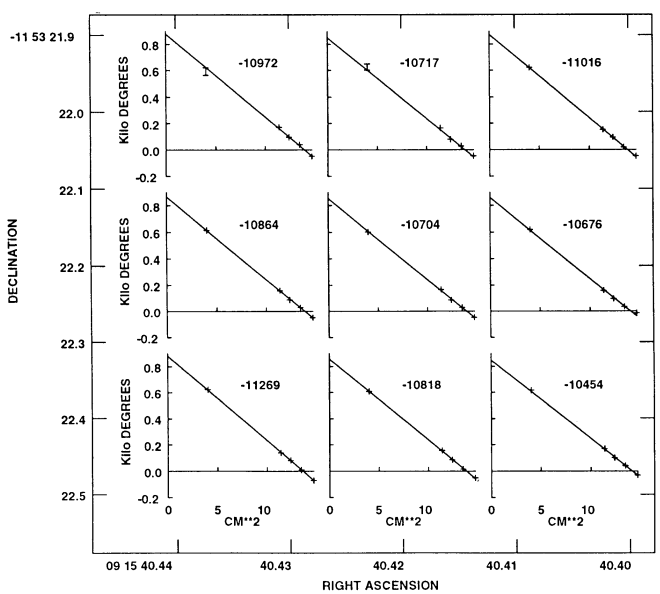

FIG. 2.—Sample fits of the RM to the observed polarization angle against the square of the wavelength for nine positions in the south lobe. The five frequencies used in the fit are at 7815, 8165, 8515, 8885, and 14940 MHz. Error bars for each point are plotted only when they exceed the size of the plotted point.

3.1. *Interstellar Medium of the Milky Way Galaxy*

Typical RMs in extragalactic sources are on the order of 0–300 radians m^{-2}, with a strong correlation with Galactic latitude (Simard-Normandin, Kronberg, & Button 1981). These RMs are well modeled by the large-scale ordered magnetic field within the Milky Way. Hydra A has a Galactic latitude of 25°.1, so the expected Galactic contribution of 0–60 radians m^{-2} is insignificant.

3.2. *Intergalactic Medium*

Vallée (1990) recently searched the catalog of Broten, Macleod, & Vallée (1988) of 674 extragalactic radio sources for a redshift dependent contribution to Faraday rotation. His result of less than 2 radians m^{-2} indicates no significant Faraday rotation, and places an upper limit on the intergalactic magnetic field of $B_{IGM} < 6 \times 10^{-11}$ G for an IGM density of 10^{-6} cm^{-3} (assuming that there are no magnetic field reversals).

3.3. *Intracluster Medium*

The ICM is now widely recognized to be a strong source of X-ray emission. This X-ray emission has been well modeled by thermal bremsstrahlung from a hot, $\sim 5 \times 10^7$ K, gas. The high-RM galaxies have a strong tendency to be found in dense, luminous X-rays clusters. The average core radius and density of the hot cluster gas in the high-RM sources for which good X-ray data exists are ~ 130 kpc and 0.01 cm^{-3} (Taylor 1991). If this plasma is magnetized, then the observed Faraday rotation measures could be produced as the radio emission travels through the ICM. For a constant longitudinal magnetic field of 3 μG, the Faraday rotation produced is 3200 radians m^{-2}. For the high-RM sources like Hydra A, this is most likely the dominant mechanism. Further discussion, in particular some possible field geometries for the ICM, is presented in § 4.

3.4. *The Optical Line Emitting Gas*

Brightest cluster galaxies in strong cooling flows, such as Hydra A, 3C 295 and Cygnus A, exhibit an excess of nonnuclear emission-line luminosities when compared with typical field radio galaxies of the same radio power (Heckman et al. 1989). Cowie et al. (1983) has observed extensive optical line emission in the cooling flow cluster A 1795. The electron densities of the line emitting gas can be quite high (e.g., 170 cm^{-3} for A1795; Heckman et al. 1989), and if a magnetic field exists then a significant RM could be produced. Optical line observations (Baum et al. 1988) show, however, that the covering factor (the fraction of the radio source coincident with line emission) for most radio sources is low, probably less than 10%. Observations of the line emitting gas in Hydra A (Baum et al. 1988) indicate that the line emission occurs only in the inner 15″ (21 kpc) of Hydra A, while the radio emission, and high RMs are more widely distributed over 80″ (110 kpc). Estimates for the volume filling factors of the line emitting gas are also low, typically 10^{-5} to 10^{-6} (Heckman et al. 1989). Ge & Owen (1993) observe that the radio source in A1795 is depolarized at 3.6 cm coincident with regions of strong optical line emission while elsewhere high RMs are observed without depolarization. Ge (1991) has interpreted this depolarization to result from Faraday rotation being produced within narrow filaments, much smaller than the telescope beam. Given these observational results, and that the emission-line gas is probably highly filamentary, it seems unlikely that the emission-line

gas could give rise to the well-ordered, coherent RMs observed.

3.5. *A Cocoon around the Radio Source*

Bicknell, Cameron, & Gingold (1990, hereafter BCG) have suggested that the high RMs observed in Cygnus A may be produced within a mixing region of entrained cluster gas and source magnetic fields around the radio emitting plasma. BCG have performed numerical simulations which show that large-scale surface waves can form out of Kelvin-Helmholtz instability waves on the lobes of radio sources. BCG hypothesize that these waves mix the magnetic fields within the source with surrounding thermal material in a way that preserves the order of the magnetic fields. The predictions of this model for Hydra A and the other high RM sources will be discussed in Taylor & Perley (1993). Briefly, this model fails to produce the required RMs in Hydra A because (1) the RMs measured in both of the jets of Hydra A are similar in magnitude to measurements of the RM in the lobes. This demands that the mixing process occur equally for the jets and lobes, which most likely have quite different field strengths, bulk velocities, etc. (2) The BCG model naturally predicts similar RMs in each lobe and therefore cannot explain the RM asymmetry between the north and south lobes of Hydra A. (3) The magnetic fields in the lobes of Hydra A are half those in Cygnus A while the observed RMs are up to three times larger. In the BCG model this requires either a much thicker Faraday screen (which implies mixing waves of a size approaching size of the lobes) or amplification of the source magnetic fields.

3.6. *Within the Radio Source*

If there is sufficient ionized, thermal gas intermixed with the radio emitting plasma, then the magnetic fields of the source may induce considerable internal Faraday rotation. Burn (1966) predicts for internal Faraday rotation that the polarization angle will obey a λ^2 law of rotation over at most 90°. Our observations (see Fig. 2) display a λ^2 law of rotation over several hundred degrees in Hydra A, ruling out a significant contribution to the RMs from internal Faraday rotation. Also, for reasonable source geometries any significant Faraday rotation will be accompanied by severe depolarization (Burn 1966). In this case, one would expect the RM to correlate with the depolarization. No correlation between RM and depolarization is evident in Hydra A (Taylor 1991).

4. MODELS FOR CLUSTER MAGNETIC FIELDS

In this section we present the various physical models involving cluster magnetic fields that have been invoked to explain high rotation measures observed in some sources. We then compare predictions of each model with the observations, particularly those of Hydra A. Hydra A is an excellent benchmark for the various models due to the extent over which we have good determinations of the RM (110 kpc) and the large absolute values of these RMs (up to 12,000 rad m^{-2}).

4.1. *Tangled Cells*

The observed RM distribution across both Hydra A and 3C 295 (Perley & Taylor 1991) has a patchy appearance. Similar RM distributions in other high RM sources, especially that of Cygnus A, have prompted Dreher et al. (1987), and Tribble (1991) to model the Faraday screen with a tangled magnetic field. In the simplest form of this model, cells of uniform size and magnetic field strength, but with fields oriented randomly in any direction are distributed throughout the ICM. The observed RM along any given line of sight will therefore be generated by a random walk process. The contribution from each cell is

$$\Delta \mathrm{RM} = 812 n_e B l \cos\theta \text{ rad m}^{-2}, \quad (1)$$

where n_e is the electron density in cm^{-3}, B is the magnetic field strength in μG, and θ is the angle between the field and the line of sight. Assuming a random distribution for θ results in an average value for the RM along a line of sight of

$$\langle \mathrm{RM} \rangle = 812 n_e B l \langle \cos\theta \rangle \text{ rad m}^{-2} = 0. \quad (2)$$

The dispersion in the rotation measure is given by

$$\langle \mathrm{RM}^2 \rangle^{1/2} = \tfrac{1}{3} 812 n_e B N^{1/2} l \text{ rad m}^{-2}, \quad (3)$$

where N is the number of cells along the line of sight. Thus, the distribution of the RM is a Gaussian with zero mean and variance given by equation (3).

Lawler & Dennison (1982) examined Faraday rotation by a tangled cluster medium in a similar analysis. Instead of a constant density, as we have assumed above, Lawler & Dennison used a King model (King 1966) of the form

$$n_e = \frac{n_0}{(1 + r^2/a^2)^{3/2}}, \quad (4)$$

where n_0 is the central electron density, and a is the core radius of the gas distribution. For this density profile, and a randomly directed magnetic field, they found

$$\langle \mathrm{RM}^2 \rangle^{1/2} = \frac{812(2\pi)^{1/2}}{4} \frac{n_0 B M^{1/2} l}{(1 + r^2/a^2)^{5/4}} \text{ rad m}^{-2}, \quad (5)$$

where M is the number of cells per core radius. Kim et al. (1990) applied the analysis of Lawler & Dennison to their observations of the Coma cluster where they measured a Faraday dispersion of 40 radians m^{-2}. Choosing l in the range 10–40 kpc, they found 25 ± 15 cells per core radius and a magnetic field strength of 1.7 ± 0.9 μG. These large magnetic field strengths require that the fields be extremely tangled since the Faraday rotation measures do not exceed 70 rad m^{-2} in Coma.

To test the predictions of the distributed cell model we have made histograms of the north lobe (Fig. 3) and south lobe (Fig. 4) of Hydra A. To exclude erroneous RM values from the histograms we blanked those RMs with errors in the polarization angle $>20°$, and at any point where the brightness of the source was less than 4.9 mJy arcsec^{-2} at 3.6 cm. The north lobe has

$$\langle \mathrm{RM} \rangle_n = 820 \text{ rad m}^{-2}, \quad \langle \mathrm{RM}^2 \rangle_n^{1/2} = 1200 \text{ rad m}^{-2},$$

where we have estimated the Faraday dispersion from the measured FWHM of the RM distribution. The nonzero mean of this distribution does not agree with the predictions of the simple distributed cell model. To explain the nonzero mean requires a contribution to the RM by a larger scale magnetic field. Assuming a path length equal to the cluster core radius of 150 kpc, and a constant density of 0.008 cm^{-3} requires, from equation (3), a magnetic field strength of 0.84 μG in the uniform component. Taking the cell size from the observed transverse coherence length in the RM distribution of $\sim$4 kpc (see § 2), results in $N = 40$ cells, and requires from equation (3), assuming a measurement error in the RM dispersion of 100 rad

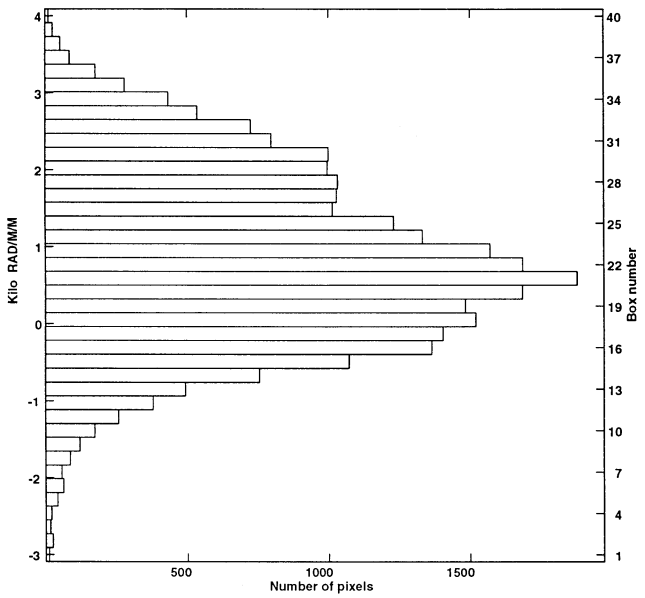

FIG. 3.—A histogram of the RM distribution of the north lobe of Hydra A. The mean of the distribution is 820 radians m^{-2}, and the dispersion is 1200 radians m^{-2}.

m^{-2}, a magnetic field strength of 22 ± 2 μG in the random component. Employing a King model for the thermal gas distribution yields (from equation [5]) a field strength of 12 ± 1 μG. This magnetic field strength is an order of magnitude larger than is found in the Coma cluster (Kim et al. 1991). The RM distribution may be broadened by gradients is an underlying, uniform magnetic field, but measurements of the Faraday dispersion throughout Hydra A indicate Faraday dispersions of 800–1500 radians m^{-2}, nearly two orders of magnitude greater than that found in Coma.

The RM distribution in the south lobe is even more non-Gaussian with a mean and dispersion of

$$\langle \mathrm{RM} \rangle_s = -3450 \text{ rad m}^{-2}, \quad \langle \mathrm{RM}^2 \rangle_s^{1/2} = 1500 \text{ rad m}^{-2},$$

and a bump in the RM distribution is clearly visible at -8000 rad m^{-2}. The larger RM dispersion is expected since the RM distribution in the south lobe is patchier, and sign reversals are more commonplace than in the north lobe. Ignoring the bump in the RM distribution for the moment, we can once again estimate the Faraday dispersion from the measured FWHM of the RM distribution. Applying a distributed cell model with an additional uniform magnetic field component, as done above for the north lobe, results in a uniform field of -3.5 μG, and a random component of 27 ± 3 μG.

A simple isotropic model predicts similar values in both the north and south lobes of Hydra A for the random magnetic field component, while the results above give different values in the lobes. This discrepancy can be removed by tipping the source, and restricting the extent, R, of the magnetized cluster halo such that many more cells are encountered along the path to the south lobe than to the north lobe. To keep the random component of the magnetic field strength the same for both lobes requires a factor of 1.6 more cells along the path to the south lobe. This can be accomplished by tipping the source 30° out of the plane of the sky, and $R = 70$ kpc. Other possible combinations of R and θ are shown in Fig. 5.

These observations of the RM asymmetry in Hydra A are consistent with the finding of Laing (1988) that the lobe on the side of the stronger jet of radio galaxies and quasars shows less depolarization. Garrington, Conway, & Leahy (1991) found 34 out of 37 F-R II sources show less depolarization on the jetted side. This would indicate that radio lobes in these sources are frequently surrounded by a magnetized plasma and that Doppler beaming is responsible for the apparent one-sidedness of their jets. For the magnetized halo to be effective in creating the depolarization asymmetry, Garrington & Conway (1991)

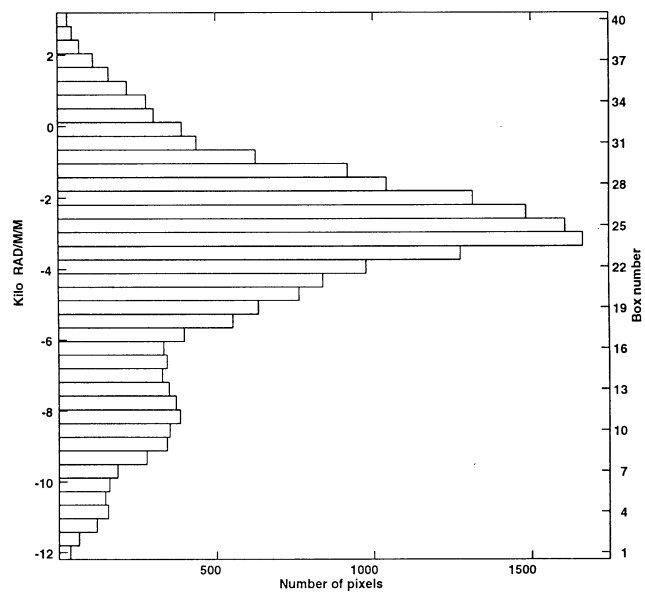

FIG. 4.—A histogram of the RM distribution of the southern lobe of Hydra A. The mean is -3450 radians m^{-2}, and the dispersion is 1500 radians m^{-2}. Note the presence of a significant bump in the RM distribution at -8000 radians m^{-2}.

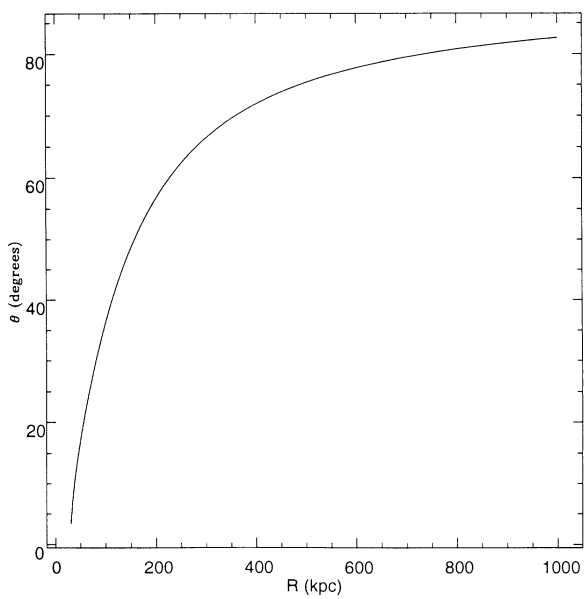

FIG. 5.—Possible combinations of the angle out of the plane of the sky, θ, and the size of the magnetized halo, R, which produce a path length through the south lobe 1.6 times that to the north lobe.

have put limits on the size of the magnetized halo to within a factor of 2 of the source size (~100 kpc). This size for the magnetized halo is similar to what we obtain for Hydra A (for $\theta < \sim 60°$) and is considerably smaller than the cluster size, but comparable to the cluster core radius. It may be that only the central region of the cooling flow cluster gives rise to the high RMs.

4.2. *Tangled Cells and a Uniform Disk*

No random distribution of cells can produce the observed large-scale structure in the RM distribution of Hydra A. For that reason we consider a model with a magnetic field consisting of both a uniform component as well as a distribution of cells with a randomly oriented magnetic field (see Fig. 6). We attempt to model the distribution of the large-scale magnetic field by analyzing the $\langle RM \rangle$ and $\langle RM^2 \rangle^{1/2}$ as a function of the projected radius.

Without knowing the inclination of Hydra A, we can only measure the projected radial distribution of $\langle RM \rangle$ and $\langle RM^2 \rangle^{1/2}$. This was done by rotating the source until it was oriented north-south, and then taking thin east-west rectangular bins over the south with a 10 pixel (1 kpc) separation. The average RM, $\langle RM \rangle$, in each bin is plotted in Figure 7. An obvious feature in Figure 7 is the large deviation 30 kpc from the core in the south lobe. This region shows up clearly in the RM image itself (Fig. 1) and is quite coherent over 5″ (7 kpc). Another clear trend is the change in sign of the RM from the north to the south lobe.

To match the observations, any model of the large-scale cluster magnetic field must change sign between the north and south lobes. The simplest such model is a circular field, similar to those observed in some spiral galaxies (e.g., M51, IC 342; Beck 1987).

For a linear source, the path length, p, through a spherical halo as a function of the projected radial distance from the center, y, is given by

$$p = \sqrt{R^2 - y^2} - y \tan(\theta) , \tag{6}$$

where R is the radius of the magnetized halo, and θ is the angle between the radio axis and the plane of the sky. Negative values of y are used for the south lobe. The component of the magnetic field parallel to the line of sight at any point along the path to the source, z, is

$$B(z) = B_u \frac{u}{\sqrt{y^2 + z^2}} , \tag{7}$$

where B_u is the strength of the uniform component of the magnetic field. The resulting RM along a line of sight is given by

$$\mathrm{RM} = 812 n_e B_u y \int_f^g \frac{y}{\sqrt{y^2 + z^2}} dz \ \mathrm{rad\ m^{-2}} . \tag{8}$$

where the lower and upper limits of the integration are

$$f = y \tan(\theta) , \quad g = \sqrt{R^2 - y^2} . \tag{9}$$

Integrating equation (9) yields the predicted RM as a function of y,

$$\mathrm{RM} = 812 n_e B_u y \left[\ln \left(\frac{g + \sqrt{g^2 + y^2}}{f + \sqrt{f^2 + y^2}} \right) \right] \mathrm{rad\ m^{-2}} . \tag{10}$$

This model was fitted to the data by finding the values of B_u, R, and θ for which χ^2 was minimized. The minimization was performed using the downhill simplex method described in Press et al. (1987, p. 289). The best-fit value of $\chi^2 = 179$, for 92 d.o.f. was found for $B_u = 5.7$ μG, $R = 76$ kpc, and $\theta = 48°$. The best-fitting model is plotted against the data in Figure 7, along with models having B_u equal to 3 and 9 μG in order to illustrate the dependence of the model on B_u. Figures 8 and 9 illustrate the dependence of the model on R and θ. This disk model reproduces the overall trends in the data fairly well, but fails to match the large deviation in RM in the south lobe.

The dispersion, $\langle RM^2 \rangle^{1/2}$, resulting from a distribution of tangled cells, is plotted in Figure 10. The best-fit values of $R = 76$ kpc and $\theta = 48°$ found above were assumed. Models for the random component of the magnetic field strength of 20, 30, and 40 μG are plotted against the data in Figure 10. The

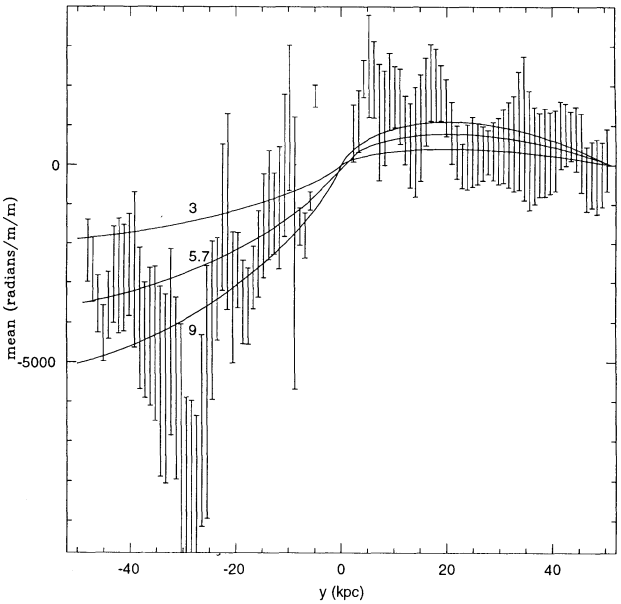

FIG. 7.—A plot of $\langle RM \rangle$ in Hydra A with projected radial distance from the core. Negative values for the distance correspond to locations in the south lobe. The solid curves represents a uniform disk magnetic field model with $B_u = 3$, 5.7, and 9 μG. The value of χ^2 for the three fits is 237, 179, and 272.

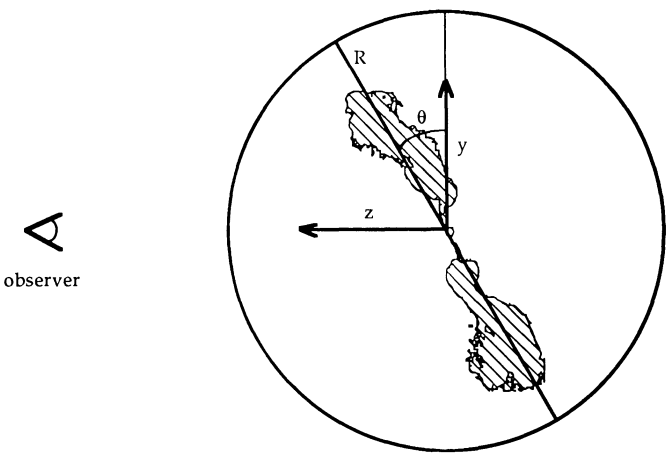

FIG. 6.—A schematic of a model for the cluster magnetic field having both a random and a uniform component (tangled cells and a uniform disk).

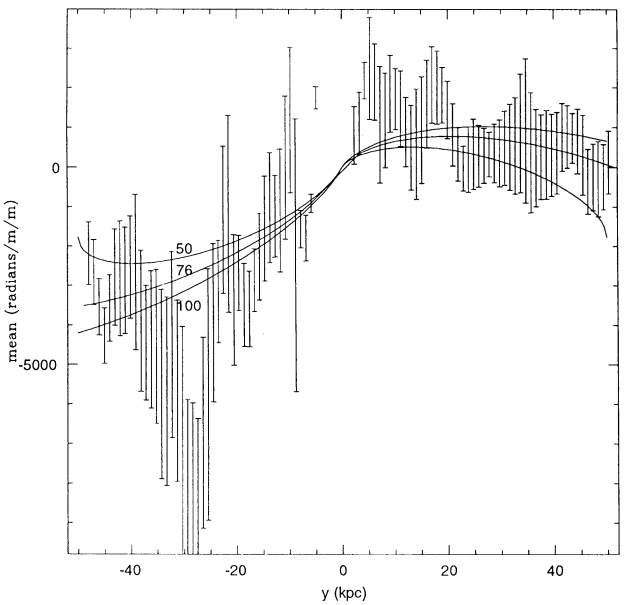

FIG. 8.—A plot of ⟨RM⟩ with projected radial distance from the core as in Fig. 7. This figure shows the variation of the model with R. For the three fits with R = 50, 76, and 100 kpc the value of χ^2 is 205, 179, and 192.

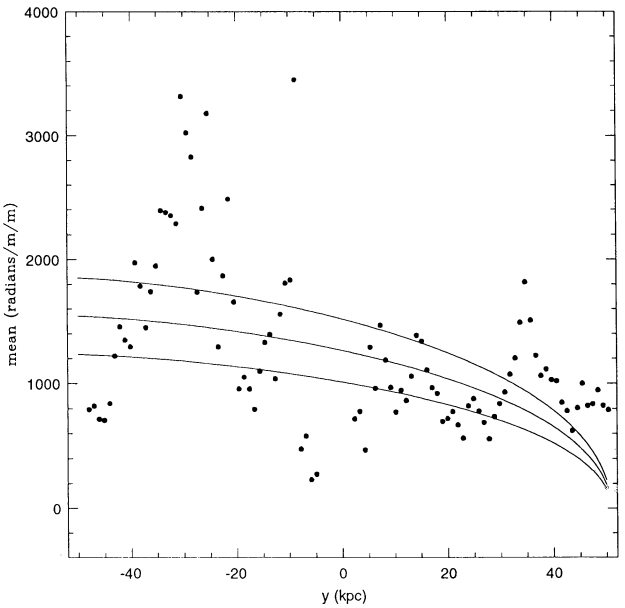

FIG. 10.—A plot of the RM dispersion, $\langle RM^2\rangle^{1/2}$, with projected radial distance from the core. Negative values for the distance correspond to locations in the south lobe. The bottom, middle, and top curves represents the expected dispersion from tangled cells of magnetic field strength 20, 30, and 40 μG along the line of sight to the source.

difference between the model in the north and south lobes comes only from the difference in path length through the magnetized halo according to equation (6). No claim is made here that this model fits the data, but as the scatter in the RM dispersion is large, a good fit will be difficult for any simple model.

4.3. *Radial Cooling Flow Field*

Soker & Sarazin (1990) predict that the central region of cooling flow clusters should exhibit high RMs, reaching 10^3–10^4 at $\sim$10 kpc. They reason that the cooling "flow" of mass into the cluster center will drag the cluster magnetic field with it, creating a highly radial field, and a magnetic field strength which varies with radius as r^{-2}. At a radius of r_B, the magnetic field pressure will equal the thermal pressure. Within this region, reconnection of the magnetic fields will occur keeping the field pressure in equipartition with the gas pressure while releasing a considerable amount of energy. This released energy may explain another of the puzzles in cooling flow clusters, where the energy to heat the line-emitting gas comes from.

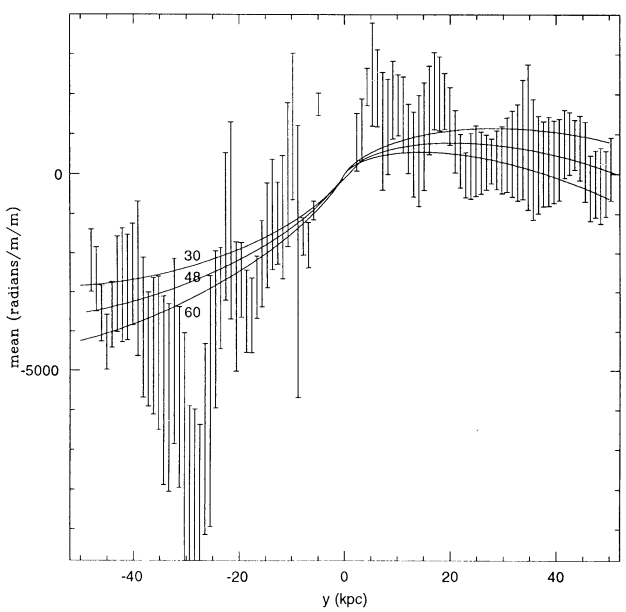

FIG. 9.—A plot of ⟨RM⟩ with projected radial distance from the core as in Fig. 7. This figure shows the variation of the model with θ. For the three fits with θ = 30, 48, and 60° the value of χ^2 is 199, 179, and 197.

Soker & Sarazin assume a density distribution $n_e \propto r^{-1}$, and an inflow velocity $v \propto r^{-1}$ for the cooling flow region. The cooling flow region has an extent r_c at which the cooling flow time reaches the age of the flow (10^{10} yr). This occurs at 100 kpc for typical cooling flow clusters, and parameters with a subscripted c refer to that radius. Soker & Sarazin assume an isotropic field outside r_c with $l_r = l_t$, where l_r and l_t are the radial and tangential coherence lengths of the tangled magnetic field. Within r_c, these coherence lengths vary as

$$l_r = l_c\left(\frac{v}{v_c}\right), \quad l_t = l_c\left(\frac{r}{r_c}\right). \tag{11}$$

The radial and tangential components of the magnetic field scale as

$$B_r = \sqrt{\frac{1}{3}}\,B_c\left(\frac{r}{r_c}\right)^{-2}, \quad B_t = \sqrt{\frac{2}{3}}\,B_c\left(\frac{r}{r_c}\right)^{-1}\left(\frac{v}{v_c}\right)^{-1}. \tag{12}$$

Outside r_B, values of $\langle RM^2\rangle^{1/2}$ as a function of projected radius, are given approximately as

$$\langle RM^2\rangle^{1/2} \approx 50\left(\frac{n_c}{3\times 10^{-3}\ \mathrm{cm}^{-3}}\right)\left(\frac{B_c}{1\ \mu\mathrm{G}}\right)\left(\frac{l_c}{10\ \mathrm{kpc}}\right)^{1/2} \times \left(\frac{r_c}{100\ \mathrm{kpc}}\right)^{1/2}\left(\frac{r}{r_c}\right)^{-2}\ \mathrm{rad\ m^{-2}}. \tag{13}$$

The location of the equipartition radius is given by

$$r_B \approx 9\left(\frac{B_c}{1\ \mu\mathrm{G}}\right)^{1/2}\left(\frac{n_c}{3\times 10^{-3}\ \mathrm{cm}^{-3}}\right)^{-7/12} \times\left(\frac{T_c}{7\times 10^7\ \mathrm{K}}\right)^{-1/4}\left(\frac{\dot{M}_c}{100\ M_\odot\ \mathrm{yr}^{-1}}\right)^{1/3}\ \mathrm{kpc}\ . \quad (14)$$

The radial model of Soker & Sarazin is very attractive in that it explains why high RM radio galaxies are found in clusters with strong cooling flows.

With the exception of Cygnus A, 3C 194, and Hydra A, the high RM sources are small in physical extent and do not permit determination of the RM outside the equipartition radius, r_B. Therefore these sources do not test the predictions of the Soker and Sarazin model. For Hydra A, however, r_B is ~ 20 kpc, while the largest RMs are found at 30 kpc. Furthermore, as can be seen in Figures 9 and 10, neither the mean or dispersion of the RM scales as r^{-2} as predicted. Another prediction of the radial field model of Soker & Sarazin is that the coherence lengths should be quite different in the radial and tangential directions (see eqs. [11] and [12]). A consequence of this is that the RMs should vary more rapidly in the tangential direction than in the radial direction. While this is difficult to estimate from RM observations, in Hydra A the coherence length appears to be isotropic, in contradiction to the prediction of the radial field model. Tribble (1993) claims that turbulent stirring will isotropize the magnetic field (and thereby eliminate the prediction of anisotropic RMs) since the turbulent velocity is much greater than the inflow velocity.

4.4. *Cluster Dynamo*

Jaffe (1980) proposed that magnetic fields in clusters could be generated by turbulence in the wakes of member galaxies. Eilek (1993) has further explored the possibility of a turbulent dynamo at work in clusters. Helical turbulence can build large-scale magnetic fields provided there exists a driving force and seed magnetic fields. The motions of galaxies through the ICM could provide the necessary driving force. Seed magnetic fields can be very small. Either a remnant primordial magnetic field or the magnetic fields stripped out of galaxies could provide the necessary seed fields.

Eilek has found many possible modes, n, for the solutions to the steady state dynamo. The averaged magnetic field is given by

$$\begin{aligned} B(r) &\propto r^{-1}\ , \quad r > r_{\max}\ ; \\ B(r) &\propto r^{n-1}\ , \quad r < r_{\max}\ . \end{aligned} \quad (15)$$

where $r_{\max} \sim 0$ for $n = 1$, and $r_{\max} \sim 1.3n\lambda_D$ for $n > 1$. The magnetic field consists of helical structures, wrapped into a "donut." Fluctuations in the RM should occur on the scale length, λ_D, where $\lambda_D = 20$ kpc for $\lambda_t = 10$ kpc.

In the steady state, the energy in the magnetic field, E_B, should be in equipartition with the energy in the turbulence, E_t. This provides an estimate for the magnetic field strength

$$B \approx \sqrt{4\pi\rho v_t^2}\ , \quad (16)$$

which, in terms of physical quantities of interest, becomes

$$B \approx 1.5\left(\frac{n_0}{10^{-3}\ \mathrm{cm}^{-3}}\right)^{1/2}\left(\frac{v_t}{100\ \mathrm{km\ s}^{-1}}\right)\mu\mathrm{G}\ . \quad (17)$$

From equation (17) we see that turbulent velocities on the order of 100–3000 km s^{-1} are needed in clusters where high RMs have been measured. Eilek points out that there may be evidence for such turbulence in observations of the kinematics of emission-line clouds. Heckman et al. (1989) suggests velocity gradients of ~ 200 km s^{-1} observed in cooling flow clusters could be due to turbulence.

Eilek has generated simulated RM images from the dynamo model. In many ways these simulations compare favorably with the observations of the high RM sources. In these simulations, the maximum in the RM does not occur in the center of the cluster, but is displaced by $1.3n\lambda_D$, or ~ 50 kpc for $n = 2$. The simulations show adjacent positive and negative patches, such as are seen in several places in Hydra A and 3C 295. Some simulations also show a change in sign of the RM across the cluster center as is seen in Hydra A.

5. DISCUSSION

While cluster magnetic fields present the most likely explanation for the high RMs found in Hydra A and the other high RM sources, the simplest models of a constant, or tangled, magnetic field distribution cannot match the observations. The more complicated disk model (§ 4.2) that we propose meets with some success in explaining the RM distribution in Hydra A, but it is purely an ad hoc model and the origin for such a structure is unclear. Furthermore, no evidence is seen in optical (Taylor 1991), or X-ray (Taylor & Perley 1993) for such a large-scale disk.

Eilek (1993) has demonstrated that a cluster dynamo can generate large-scale cluster magnetic fields (§ 4.4). Cluster dynamo models require a small seed magnetic field to start with. The ultimate source of the magnetic field must be in some sort of primordial magnetic field. In the case of exotic superconducting string theories the fossil magnetic fields are quite large, 10^{-9} G (Thompson 1990). In the more conventional inflationary cosmological scenarios the primordial fields created are quite negligible (Pudritz 1990). Pudritz & Silk (1989) speculate that a Biermann battery mechanism could act on rotating protogalaxies to generate seed fields of 10^{-19} G. The action of the dynamo must proceed rapidly enough to amplify this week seed field to the currently observed values of 10^{-5} G, within the Hubble time of 10^{10} yr. Pudritz & Silk (1989) point out that the dynamo process is exponential with time. The factor of 10^{14} amplification in field strength then requires $\sim 30e$-foldings. The crossing time over which this field generation takes place must then be limited to $\sim 3\times 10^8$ yr. For realistic velocities of galaxy motion, this limits the cluster dynamo action to roughly the central 200 kpc, coincidentally the cluster core radius. The constraints from depolarization asymmetries found by Garrington & Conway (1991), and the RM asymmetry in Hydra A discussed in § 4.2, suggest that the extent of many cluster magnetic fields may be limited to the core radius in extent.

The cluster magnetic fields could be remnant magnetic fields of extinct radio galaxies. Rich clusters often have several head-tail radio galaxies within them (e.g., 5C 4.81, 5C 4.85, and others in the Coma cluster; Kim et al. 1990). The central engines for such sources could turn off, causing the radio emission to fade and leaving behind both large-scale magnetic fields and a random component in the cluster. Both large- and small-scale magnetic fields are required to reproduce the RM distribution observed for Hydra A.

Magnetic fields could also be stripped from spiral galaxies. This is consistent with the theory of galactic cannibalism in which giant elliptical galaxies, such as are found at the center of cooling flow clusters, have grown through capturing member galaxies. This has been used to explain the low fraction of spiral galaxies found in the centers of dense clusters (Butcher & Oemler 1978). In the merging process, the magnetic fields of the spiral galaxies, with typical strength 3 μG and scale 10 kpc, could be tangled and distributed through the cluster. These mergers could also be a source for the hot cluster gas. Observations of iron lines in the hot cluster gas indicate that the hot gas cannot all be of primordial origin. To speculate even further, the very presence of the radio galaxy at the heart of the cooling flow may be the result of these mergers. There is some evidence (Roos 1985) that mergers induce condensations in the galaxy cores which may fuel an active nucleus.

Numerical simulations by De Young (1992), have shown that in general galaxy-driven turbulence has considerable difficulty producing cluster magnetic fields of the observed strengths and scales. He concludes that cluster magnetic fields will be rare, present only in the cores of rich clusters when special conditions exist. These conditions (many of which are discussed above) are cooling flows, the presence of a luminous radio source, a previous generation of strong radio sources, and merging. We suggest that the strong magnetic fields found in the high RM sources are linked to the presence of the cooling flow which has both enhanced the efficiency of the magnetic dynamo and amplified the fields within the central region by adiabatic compression.

The study of the RMs in higher redshift objects may lead us to an improved understanding of cluster evolution. Many compact steep spectrum sources exhibit a high integrated RM, but even large synthesis telescopes like the VLA can tell us little about their RM distribution. The Multi-Element Radio Linked Interferometer (MERLIN) telescope at Jodrell Bank has been reoutfitted. With baseline lengths up to 10 times that of the VLA in its largest configuration, MERLIN should be capable of the sensitive, high-resolution polarimetry needed to map the RM distribution of compact steep spectrum sources (such as 3C 318; Taylor, Inoue, & Tabara 1992b). If we continue to find high RMs at large redshifts, this may indicate the presence of a denser cluster medium, or even stronger cluster magnetic fields, in the early universe. The new VLBA (Very Long Baseline Array) telescope is also nearing completion. Sensitive polarimetry should be possible with the VLBA at resolutions up to 1 mas at 6 cm. The VLBA will also be a useful instrument for investigating the polarization properties and RM distribution of compact steep spectrum sources. In addition, the VLBA could be used to investigate the RM distribution of parsec-scale radio jets, and thereby probe the environment around active galactic nucleii.

6. CONCLUSIONS

The observations of high Faraday rotation measures in Hydra A can most reasonably be explained by the presence of cluster magnetic fields. Observations of the RM distributions of Hydra A and 3C 295 (Perley & Taylor 1991) indicate that sign reversals are common, and the correlation length appears to be $\sim$4 kpc. The strength of the tangled component of the magnetic field is $\sim$30 μG in Hydra A. Furthermore, the large-scale order that we observe for the Faraday rotation implies that these magnetic fields are at least partially ordered on scales of 100 kpc.

Several theories to explain the high RM radio sources have considerable difficulties when confronted with the new observations. The mixing layer model of BCG cannot explain the high RMs observed in Hydra A, or the asymmetry, or the high RMs of the jets. A simple model of the cluster magnetic field as a collection of tangled cells cannot reproduce the observed RM distribution. In particular, the nonzero mean for the RM distribution requires a substantial magnetic field ($\sim$6 μG), to be ordered over a large scale ($\sim$100 kpc). The predictions of the radial inflow model of Soker & Sarazin (1990) do not appear to be borne out by the observations.

We have formulated a model consisting of a large-scale ordered component of the magnetic field in the shape of a disk. The best-fitting parameters for this model applied to our Hydra A data are a uniform magnetic field of strength 5.7 μG, disk radius 76 kpc, source inclination angle of 48°, and a random magnetic field component of strength 30 μG. This model meets with some success in explaining the observed RM distribution, but the physical basis for such a large-scale disk is unclear. No other evidence, either in optical or X-ray observations suggests that such a structure might be present. Alternatively, the dynamo model of Eilek (1993) holds considerable promise for explaining both the observed small- and large-scale structure observed in the Faraday RMs.

The authors have benefited from discussions with J. A. Eilek, J.-P. Ge, F. N. Owen, and J. O. Burns. One of us (G. B. T.) would like to acknowledge support for this research from an NRAO predoctoral fellowship, and from NSF under grant AST-9117100.

REFERENCES

Baum, S. A., Heckman, T. M., Bridle, A. H., van Breugel, W. J. M., & Miley, G. K. 1988, ApJS, 68, 643
Beck, R. 1987, in Magnetic Fields and Extragalactic Objects, ed. E. Asséo & D. Grésillon (Les Ulis: Editions de Physique), 113
Bicknell, G. V., Cameron, R. A., & Gingold, R. A. 1990, ApJ, 357, 373 (BCG)
Broten, N. W., Macleod, J. M., & Vallée, J. P. 1988, Ap&SS, 141, 303
Burn, B. F. 1966, MNRAS, 133, 67
Butcher, H., & Oemler, A. 1978, ApJ, 226, 559
Cowie, L. L., Hu, E. M., Jenkins, E. B., & York, D. G. 1983, ApJ, 272, 29
De Young, D. S. 1992, ApJ, 386, 464
Dreher, J. W., Carilli, C. L., & Perley, R. A. 1987, ApJ, 316, 611 (DCP)
Eilek, J. A. 1993, in preparation
Garrington, S. T., & Conway, R. G. 1991, MNRAS, 250, 198
Garrington, S. T., Conway, R. G., & Leahy, J. P. 1991, MNRAS, 250, 171
Ge, J. P. 1991, Ph.D. thesis, New Mexico Inst. of Mining and Technology
Ge, J. P., & Owen, F. N. 1993, AJ, 105, 778
Heckman, T. M., Baum, S. A., van Breugel, W. J. M., & McCarthy, P. C. 1989, ApJ, 338, 48
Jaffe, W. 1980, ApJ, 241, 925
Kim, K.-T., Kronberg, P. P., Dewdney, P. E., & Landecker, T. L. 1990, ApJ, 355, 29
King, I. R. 1966, AJ, 71, 64
Laing, R. A. 1988, Nature, 331, 149
Lawler, J. M., & Dennison, B. 1982, ApJ, 252, 81
Perley, R. A., & Taylor, G. B. 1991, AJ, 101, 1623
Press, W. H., Flannery, B. P., Teukolsky, S. A., & Vetterling, W. T. 1987, Numerical Recipes (Cambridge: Univ. Press)
Pudritz, R. E. 1990, in IAU Symp., Galactic and Intergalactic Magnetic Fields, ed. R. Beck et al. (Dordrecht: Kluwer), 519
Pudritz, R. E., & Silk, J. 1989, ApJ, 342, 650
Roos, N. 1985, ApJ, 294, 479
Sarazin, C. L. 1986, Rev. Mod. Phys., 58, 1

Simard-Normandin, M., Kronberg, P. P., & Button, S. 1981, ApJS, 45, 97
Soker, N., & Sarazin, C. L. 1990, ApJ, 348, 73
Taylor, G. B. 1991, Ph.D. thesis, University of California, Los Angeles
Taylor, G. B., Inoue, M., & Tabara, H. 1992a, A&A, 264, 415
———. 1992b, A&A, 264, 421
Taylor, G. B., & Perley, R. A. 1993, in preparation
Taylor, G. B., Perley, R. A., Inoue, M., Kato, T., Tabara, H., & Aizu, K. 1990, ApJ, 360, 41
Thompson, C. 1990, in IAU Symp. 140, Galactic and Intergalactic Magnetic Fields, ed. R. Beck et al. (Dordrecht: Kluwer), 507
Tribble, P. C. 1991, MNRAS, 250, 726
———. 1993, MNRAS, submitted
Vallée, J. P. 1990, ApJ, 360, 1